ISM abundances and history: a 3D, solar neighborhood view

R. Lallement[1], J.-L. Vergely[2], L. Puspitarini[1]

[1] GEPI Observatoire de Paris, CNRS, Université Paris Diderot, Place Jules Janssen 92190 Meudon, France e-mail: [rosine.lallement;lucky.puspitarini]@obspm.fr

[2] ACRI-ST, 260 route du Pin Montard, Sophia Antipolis, France

Abstract. For observational reasons, the solar neighborhood is particularly suitable for the study of the multi-phase interstellar (IS) medium and the search for traces of its temporal evolution, however by a number of aspects it seems to be a peculiar region. Using recent 3D maps of the IS dust based on color excess data, as well as gas distributions, we illustrate how maps can shed additional light on the specificity of the local medium, its history and abundance pattern.

3D maps reveal a gigantic cavity located in the third quadrant and connected to the Local Bubble, the latter itself running into an elongated cavity toward $l \simeq 70°$. Most nearby cloud complexes of the so-called Gould belt but also more distant clouds seem to border a large fraction of this entire structure. The IS medium with the large cavity appears ionized and dust-poor, as deduced from ionized calcium and neutral sodium to dust ratios. The geometry favors the Olano scenario of Gould belt-Local Arm formation through the braking of a supercloud by interaction with a spiral density wave. The highly variable D/H ratio in the nearby IS gas may also be spatially related to the global structure. We speculate about potential consequences of the supercloud encounter and dust-gas decoupling during its braking, in particular the formation of strong inhomogeneities in both the dust to gas abundance ratio and the dust characteristics: (i) during the $\simeq$ 500 Myrs prior to the collision, dust within the supercloud may have been gradually, strongly enriched in D due to an absence of strong stellar formation and preferential adsorption of D; (ii) during its interaction with the Plane and the braking dust-rich and dust-poor regions may have formed due to differential gas drag, the dust being more concentrated in the dense areas; strong radiation pressure from OB associations at the boundary of the left-behind giant cavity may have also helped in emptying the cavity from its dust at the profit of the central parts of the supercloud ; (iii) present D/H variations could be due to the combination of those dust inhomogeneities and posterior, localized deuterium release by grains in recent star forming regions. In this case, the *true* local D/H ratio has an intermediate value within the observed range.

Key words. Galaxy:Interstellar medium - Galaxy:abundances

1. Introduction

Multiwavelength InterStellar Medium (ISM) emission surveys have provided very detailed

maps of interstellar matter in the Galaxy, however they lack precise information on the distance to the emitting clouds. On the other hand, 3D ISM distributions require distance-limited measurements, gathered for huge amounts of target stars located at known, widely distributed distances. Those line-of-sight data may be either absorption features that provide absorbing columns of various species, or color excess measurements that provide dust columns. To date, a small series of maps of the nearby ISM have been produced based on a robust tomographic inversion of individual stellar data (Tarantola & Valette, 1982). They are currently based on lines of NaI and CaII (Vergely et al. (2001); Lallement et al. (2003); Welsh et al. (2010) and color excess measurements (Vergely et al. (2010); Lallement et al. (2014),). NaI traces dense and neutral IS, CaII traces both dense neutral and ionized gas, while extinction traces the dust in all phases. However, as demonstrated by recent works, one may expect significant progresses in those 3D maps. First, diffuse interstellar bands (DIBs) are available as IS clouds tracers and may advantageously complement NaI and CaII for distant and reddened targets (Raimond et al., 2012; Chen et al., 2013; Puspitarini et al., 2013; van Loon et al., 2013). Both absorption lines and DIBs have the unique advantage of being directly linked to emission spectra through their Doppler shifts (e.g. Puspitarini & Lallement, 2012). Second, the number of potential target stars increases considerably with the introduction of fitting methods based on synthetic stellar spectra and their application to cool stars (Chen et al., 2013). During the next decade 3D maps of increasing quality should be produced, thanks to stellar surveys of all kinds on one hand, and, hopefully, precise Gaia parallaxes on the other hand. In future, hopefully wide-field multiplex spectrographs (Bonifacio et al., 2010) will be constructed and provide massive datasets available for 3D mapping. In this work we show some aspects of the present, low resolution 3D maps of the solar neighborhood ISM. We illustrate how they may shed light on the local history, and use them to revisit the controversy about the local deuterium abundance.

2. The Galactic plane and the supercloud scenario for the Local Arm-Gould belt formation

Figure 2 taken from Lallement et al. (2014) shows the color-coded differential opacity distribution in the Galactic plane (GP), i.e. a planar cut within the three-dimensional distribution of differential opacity. We warn the reader that due to the (still) coarse grid of target stars, a smoothing length is imposed during the inversion process. Here a bi-modal spatial correlation function allowing for both high contrast, 15 pc wide and lower contrast, 25 pc wide structures is used, i.e. clouds smaller than 15 pc can not be mapped at their actual sizes. Instead, they are represented as more extended, diluted clouds. The map reveals the series of dense structures that bound the so-called Local Cavity, the $\simeq$ 100 pc wide empty region around the Sun: the Aquila, Ophiuchus, Scorpius, Lupus, Crux and Centurus dense clouds in the first and fourth quadrant, the Cassiopeia, Lacerta, Perseus, Taurus, and the closest Orion clouds in the anti-center area. Since most of these structures are not centered exactly on the GP, what appears in the cut maybe their top or bottom part. These well known structures are part of the so-called Gould belt (GB), a $\simeq$ 20° inclined, ellipsoidal chain of dense clouds and young ($\leq$10 Myrs old) O-B associations Olano (2001); Perrot & Grenier (2003); Pöppel et al. (2010). Apart from the belt Fig 2 also shows in the third quadrant a conspicuous, 500 to 1,000 pc wide cavity. This cavity can be seen as an extension at large distances of the so-called Canis Major *tunnel*, a region of rarefied gas that extends up to 130-150 pc in the direction of the stars β and ϵCMa (Gry et al., 1985). The huge cavity is centered below the Plane, and its location and extent corresponds very well to the HI 21cm super-shell GSH238+00+09, schematically represented in Heiles (1998). This peculiar super-bubble is bounded by the chain of Orion clouds on one side, and by Vela clouds at $\simeq$ 260-270 °. The whole structure, i.e. the association of the huge cavity and the Gould belt, is in favor of a scenario elaborated by Olano (2001) in an attempt to explain the Sirius su-
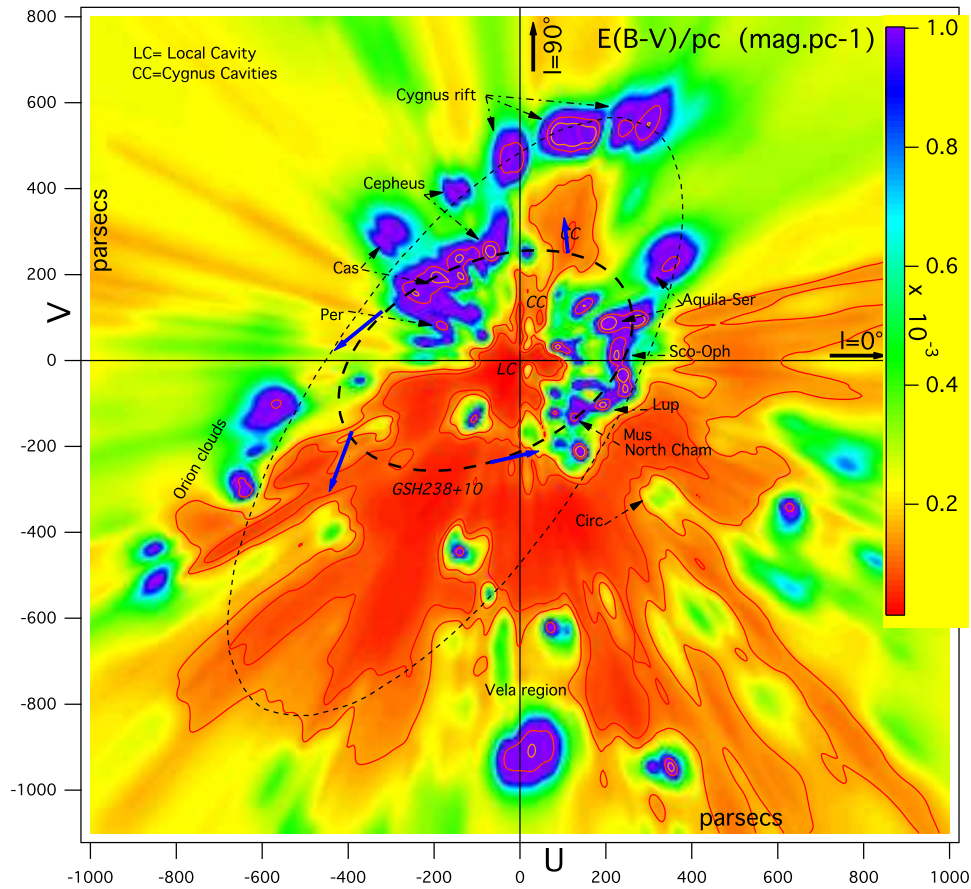
Fig. 1. Differential color excess in the Galactic plane, derived by inversion of line-of-sight data (map from Lallement et al., 2014). The Sun is at (0,0) and the Galactic center direction is to the right. Cavities (in red) are probably filled with hot (1 MK) gas or warm, tenuous ionized gas. Also shown is the Gould belt modeled by Perrot & Grenier (2003) (smaller ellipse) with four vectors (in blue) illustrating its expansion and rotation. The large ellipse represents the global structure discussed in the text and potentially associated to the supercloud braking model of Olano (2001).

percluster, the Local Arm and the inclined and rotating Gould belt. According to this model, a supercloud (SC) of size and mass on the order of 400 pc and 2 10^7 solar masses, initially moving ballistically outside the Plane and slowly rotating, has interacted with a major spiral arm ∼ 100 yrs ago. During the braking phase the old (∼ 500 Myrs or more) generation of stars from the SC decoupled from most of the gas, the central part of the SC partly collapsed to form the GB structures while keeping a global rotation, and external parts with lower angular momentum expanded and formed the Local Arm. During the last ∼ 100 Myrs young generations of stars formed and/or exploded in the compressed GB clouds, formed high pressure cavities and initiated a global expansion of the Belt. Interestingly, Olano's prediction of the formation of a large cavity left behind the braked supercloud seems to be verified here in

the dust maps. More work is needed to better assess the whole scenario, based on detailed maps and associated cloud kinematics, in combination with the stellar properties.

3. Ionization and dust abundance pattern

In the same way the IS cloud spatial distribution may help shedding light on the local history, spatial trends in abundances and/or ionization are another potential source of information. Using our database of IS neutral sodium (NaI) and ionized calcium (CaII) absorption data (presented in Welsh et al., 2010), we have attempted to compare these line-of-sight integrated columns with the color excess data. Since the absorption data involve early-type stars (used for their smooth continua), there is no overlap between the target list of this absorption database and the one of the photometric database used for the 3D map, and subsequently no possibility to compute ratios between color excess and NaI/CaII column both directly measured toward the same target. Instead, we used the coordinates and the distance of each target star for which NaI or CaII was measured, discretized the corresponding line-of-sight into distance bins on the order of our dust map grid size, and we integrated along the line-of-sight the differential opacity interpolated from the inverted 3D map (i.e. the quantity shown in Fig 1). This provides for each NaI/CaII star an estimate of the color excess. The resulting E(B-V)/N(NaI) and E(-V)/N(CaII) are represented in Fig 2a and b respectively. In figure 2a we restrict to target stars located within 100 pc from the Plane, and each target is represented by its projection onto the Plane, superimposed onto the dust distribution of Fig 1. The dust/CaII ratio shows striking differences as a function of the star location. In particular, stars in the large cavity of the third quadrant, beyond the Local Bubble, are characterized by a two to three orders of magnitude smaller dust/CaII ratio than stars located in the other quadrants at similar distances. This is a clear mark of increased ionization, dust evaporation or the well-known combination of the two effects. As a matter of fact, evaporating

dust releases a significant amount of calcium in the gas, thus the two effects contribute to the increase of the CaII/dust ratio. Such an ionization gradient pointing to the third quadrant and the CMa tunnel has already been inferred in the past, completely independently, from HI, HeI and HeII column-densities towards nearby white dwarfs (Wolff et al., 1999). These authors showed that the H ionization fraction is globally increasing along the $(l,b)=(228°,-22°)$, from ~0 at the Sun up to ~50% at 100 pc. Here it becomes clear that this trend extends further away and is amplified, i.e. the clouds embedded in the huge cavity are more strongly, probably fully ionized. This is also in line with a study of the soft X-ray background showing that the third quadrant cavity is very likely filled by a significant fraction of non X-ray emitting, warm ionized gas (Puspitarini et al., 2014).

Fig 2b displays the ratio NaI/E(B-V), for all the NaI targets, shown in projection onto a 2D sky map. Because NaI is much more concentrated spatially compared to CaII, the computed ratios are much more sensitive to the uncertainties on target distances and dust distributions. As a result of those uncertainties, there is a large dispersion of the ratios, which makes the spatial analysis more difficult than for CaII. Still, again a trend is visible: there is a smaller dust/NaI ratio in the third quadrant and especially below the Plane, compared to other directions, although this trend is less clear than for CaII (note that the same representation as the one used for CaII would look similar, although with less contrast). Such a trend is more difficult to explain than for CaII. While the high CaII/dust ratios can be explained by ionization and dust evaporation (with calcium release in the gas phase) that occur in shock-heated ionized gas, this explanation does not hold for NaI. As a matter of fact, NaI does not trace the warm ionized phase but instead the neutral clouds. In this phase the dust is not expected to have been destroyed, and, because dust contains much less sodium than calcium, in case of destruction there cannot be any significant subsequent increase of sodium in the gas phase. As a result, a small E(B-V)/NaI ratio is not likely related to dust evaporation.
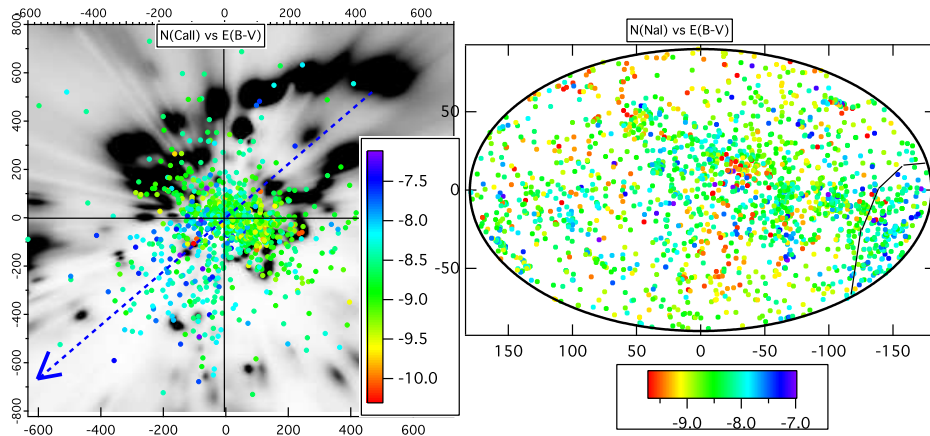
Fig. 2. Left: CaII target stars close to the GP, superimposed on the opacity map of Fig 1 (from Puspitarini et al. 2014). The color refers to the ratio between the CaII column-density measured by absorption and the color excess along the same line-of-sight, derived by line-of-sight integration through the inverted 3D distribution of differential opacity. Stars located in the third quadrant are characterized by a particularly high CaII/E(B-V) ratio. Right: Full-sky location of NaI target stars. The color refers to the ratio between the NaI column and the integrated color excess. The third quadrant, especially below the GP, is characterized by high NaI/E(B-V) ratio.

Instead, it suggests that neutral clouds in the third quadrant, embedded in (or around) the big cavity are characterized by an anomalously low dust to gas ratio. More data will be necessary to confirm this trend, that may contain additional clues about the local history.

Are the 3rd quadrant very strong ionization and dust depletion consistent with the supercloud scenario? the answer is likely yes, since during the braking large volumes of gas have been shock-heated, and thus ionized cavities with low dust are expected. On the other hand, the formation of a large scale ionization gradient such as the one we have discussed is not obvious. Is it related to the cavity that is left behind the dense part of the supercloud? Clearly discussing the formation of dust-poor gas (as evidenced by the Na/dust ratio) and a large scale ionization gradient requires detailed self-consistent modeling of gas and dust in the context of Olano's scenario. Such a model does not exist yet, and at this stage one can only speculate about some potential effects. As an example, we may hypothesize that, during the super cloud braking, inhomogeneous gas drag may have preferentially dragged the dust into the central parts that condensed to form the belt, while tenuous left-behind gas has been depleted in dust.

At this stage it is worthwhile to mention the second type of scenarios proposed for the Gould belt formation, namely the past occurrence of a series of supernovae explosions within a short time and in the same area, or the past occurrence of a unique, extremely strong explosive event such as a hypernova/gamma-ray burst. Evidently, such episodes may have preferentially ionized the gas close to the explosion sites (the third quadrant ?) and created strong ionization gradients. The radiation pressure on the dust could have have created a cavity devoid of dust and gas such as the one detected in the maps, and lower dust-gas coupling in the tenuous regions may have resulted in relatively less dust and more gas left behind during the formation of such cavities. If the explosion has occurred below the plane, directional effects of the burst could have pushed the gas

in a non-planar direction and produced an inclined structure like the Gould belt. Globally, this scenario fits also quite well the observations, including the newly found big cavity and missing dust, in addition to the ionization gradient, at the exception however of the GB rotation. The difficulty in explaining the rotation has already been discussed in previous works (Perrot & Grenier (2003) and references therein).

4. The problem of the D/H variability in the nearby IS gas

The actual value of the deuterium abundance in the local IS gas is still debated. The D/H ratio in the gas phase has been measured based on various UV spectrographs (e.g. Jenkins et al., 2000; Moos et al., 2002; Wood et al., 2004) and found to vary by a factor between 3 and 5 for target stars located mostly within about 1 kpc (Linsky et al., 2006; Prodanović et al., 2010). Interestingly, the D/H ratio is about constant for H column-densities $\leq 10^{19}$ cm^{-2}, i.e within the Local Bubble or at its boundaries. For higher columns it becomes highly variable and comprised between 5 and 20-25 ppm, while for N(H) $\geq 10^{21.5}$ cm^{-2} it seems again about constant, although the number of targets is very limited. The highest values are uncomfortably close to the primordial value measured towards quasars (Cooke et al., 2014), while the low values imply a very strong astration, above model predictions (e.g. Lagarde et al., 2012). Linsky et al (2006) suggested that the variability is due to localized release of deuterium from dust grains that are overabundant in D, due to their preferential accretion of D compared to H (see Jura, 1982; Draine, 2003). In support to this mechanism are the positive correlations they found between D/H and both FeII/H, MgII/H, that suggest that D is released along with those metals. Subsequent and quite good correlations were also found between D/H and TiII/H (Prochaska et al., 2005; Lallement et al., 2008). A contradictory view is that H columns are very uncertain and their errors create an apparent (but not real) correlation between the abundances of D and other species relative to H (e.g. Hébrard

et al., 2005). However, (Lallement et al., 2008) disfavored this argument by deriving a positive correlation between TiII/H and D/O, as well as between FeII/H and D/O. Still, the deuterium release by dust requires an extremely high D/H ratio in the dust, on the order of 0.25. This is theoretically possible for very cold dust and in dense clouds, however it requires very long periods of time without sputtering (see Linsky et al., 2006), which may be problem in the local ISM.

Another potential source of D/H variability is localized infall of pristine, highly deuterated gas and its incomplete mixing (e.g. Romano et al., 2006). At first sight it is tempting to involve the super-cloud mentioned previously as the potential progenitor of the Gould belt and the giant cavity, and consider the cloud as a source of D-rich gas. However, this is contradicted by the lack of chemical abundance inhomogeneities in the local gaseous ISM on one hand (e.g. O/H is about constant, see André et al. 2003, and carbon shows little variability, see Sofia et al. 2004), and by the absence of evidences for abundance variabilities among the nearby stars (e.g. Nieva & Przybilla, 2012), even if stars associated to the Gould belt and disk stars form distinct groups from the kinematical point of view. Note that, while this abundance homogeneity for stars and gas disfavors the infall of pristine gas, it does not disfavor the super-cloud scenario: as a matter of fact, according to Olano's scenario the super cloud is not made of pristine matter, instead the supercloud has been forming stars for at least 500 Myrs before its encounter with the Plane, and thus its IS gas has been significantly astrated.

Is there a potential link between the supercloud accretion and the D/H variability, even if the cloud is not pristine? First, we note that there is an apparent link between the D/H ratio and the global structure seen in Fig 1. As a matter of fact, if we follow Linsky et al. (2006) and divide the D/H measurements into the three categories mentioned above, the constant D/H, low HI column lines-of-sight correspond to stars within the Local Bubble, the variable D/H, intermediate column lines-of-sight correspond to target in and around the

Gould belt, and finally the low D/H, distant targets are not parts of the GB but belong to distant regions in the Local Arm. Thus, a potential link between D/H and the global structure is suggested by this correspondence. Now, the combination of the structure (the distribution of Fig 1) the ionization and the dust properties discussed above may point to the following scenario: (i) Let's assume that before its encounter/braking the supercloud in ballistic orbit has had a relatively quiet evolution during a long period of time, e.g. during the latest 500 Myrs after the formation of what is today the Sirius supercluster (see Olano, 2001). This gives a considerable amount of time for the dust to get gradually enriched in D, and alleviates one of the problems with the release scenario, namely that it requires a very long **quiet** period for the establishment of a strong concentration of D in the grains. (ii) During the cloud braking, dynamical effects result in dust-gas decoupling and in significant dust to gas ratio inhomogeneities, more dust being dragged by the densest clouds that will form the Gould belt, while more tenuous gas in the left-behind cavity or in the external parts of the supercloud loses its grains. Radiation pressure drifts may also have helped in generating large inhomogeneities in the dust to gas ratio, This alleviates in a different and additional way the problem of the required, high D/H enrichment, because the higher the dust to gas ratio, the stronger the potential release of D in the gas after dust evaporation, for the same proportions of deuterium in the grains. (iii) When, after the braking, new stars are formed in the Gould belt as a result of shocks and compressions, stellar winds and supernovae initiate the dust disruption and the release of deuterium in the gas phase, a release that is spatially inhomogeneous in a double way, due to the spatially variable dust concentration in the gas on one hand, and due to the spatially variable dust origin and deuterium content on the other hand. All those effects may have induced a significant D/H variability in the gas. From the point of view of the D/H measurements, this scenario implies that neither the highest nor the lowest values can be chosen as representative of the true local D/H ratio. Instead an average value may be the best

choice. We note that, in the frame of the explosive event and in the absence of a supercloud, strong dust to gas inhomogeneities may have been also created as a result of radiation pressure on grains and grain-gas decoupling in the more tenuous gas. In this case however, it is not possible to invoke a pre-existing D-rich dust as in the case of the super-cloud.

5. Conclusion

In this article we have attempted to illustrate the potential use of three-dimensional maps of the ISM. The cloud distribution, the ionization pattern, the dust to gas ratio contain clues about the local history of stars and gas. By some aspects the local ISM appears peculiar, in particular the existence of the inclined and expanding Gould belt, and the existence of a huge cavity devoid of dust that runs into the Gould belt, with embedded clouds being strongly ionized and dust-poor. This is in favor of the supercloud encounter and braking scenario of Olano (2001), a scenario that aims at explaining both the stellar streams, the Gould belt and the Local Arm. We considered a potential link between the local structure, ionization and dust pattern and the D/H ratio local variability, in the frame of Olano's scenario. To do so we extended one of the proposed mechanisms for D/H spatial variations, a mechanism based on dust grain evaporation (Linsky et al., 2006). Our speculated chain of events involves a strong enrichment in deuterium of the supercloud dust prior to its collision, subsequent dust-gas decoupling during the braking phase and formation of dust-rich and dust-poor areas, followed by star formation and highly inhomogeneous deuterium release in the gas through dust sputtering. This alleviates significantly and in two ways the requirement for high D/H ratio in dust grains at the basis of the dust evaporation mechanism. Alternatively, the strong explosive event scenario (e.g. a gamma-ray burst) may have initiated strong dust to gas variability, mainly through radiation pressure, but does not explain as well the dust enrichment in D. In both cases, this means that neither high nor low D/H measurements are representative of the true local D/H ratio. Instead,

the true ratio may be closer to an intermediate value. More abundance measurements, maps with higher resolution and detailed evolutionary models of stars, gas and dust are required to fully assess the local history and bring clues to the D/H problem.

References

André, M. K., Oliveira, C. M., Howk, J. C., et al. 2003, ApJ, 591, 1000

de Avillez, M. A., & Breitschwerdt, D. 2009, ApJ, 697, L158

Bonifacio, P., Arenou, F., Babusiaux, C., et al. 2010, Proc. SPIE, 77350E, 9

Chen, H.-C., Lallement, R., Babusiaux, C., et al. 2013, A&A, 550, A62

Cooke, R. J., et al. 2014, ApJ, 781, 31

Draine, B. T. 2003, ARA&A, 41, 241

Gry, C., York, D. G., & Vidal-Madjar, A. 1985, ApJ, 296, 593

Hébrard, G., Tripp, T. M., Chayer, P., et al. 2005, ApJ, 635, 1136

Heiles, C. 1998, ApJ, 498, 689

Jenkins, E. B. et al. 2000, ApJ, 538, 275

Jura, M. 1982, in Advances in Ultraviolet Astronomy, ed. Y. Kondo, NASA CP-238, 54

Lagarde, N., Romano, D., Charbonnel, C., et al 2012, A&A, 542, A62

Lallement, R., et al. 2003, A&A, 411, 447

Lallement, R., Hébrard, G., & Welsh, B. Y. 2008, A&A, 481, 381

Lallement, R., et al. 2014, A&A, 561, A91

Linsky, J. L., Draine, B. T., Moos, H. W., et al. 2006, ApJ, 647, 1106

Moos, H. W. et al. 2002, ApJS, 140, (1), 3

Nieva, M.-F., & Przybilla, N. 2012, A&A, 539, A143

Olano, C. A. 2001, AJ, 121, 295

Perrot, C. A., & Grenier, I. A. 2003, A&A, 404, 519

Pöppel, W. G. L., et al. 2010, A&A, 512, A83

Romano, D., et al. 2006, MNRAS, 369, 295

Prochaska, J. X., Tripp, T. M., & Howk, J. C. 2005, ApJ, 620, L39

Prodanović, T., Steigman, G., & Fields, B. D. 2010, MNRAS, 406, 1108

Puspitarini, L., & Lallement, R. 2012, A&A, 545, A21

Puspitarini, L., Lallement, R., & Chen, H.-C. 2013, A&A, 555, A25

Puspitarini, L., et al. 2014, A&A, in press

Raimond, S., et al. 2012, A&A, 544, A136

Sofia, U. J., et al. 2004, ApJ, 605, 272

Tarantola, A., & Valette, B. 1982, Reviews of Geophysics and Space Physics, 20, 219

van Loon, J. T., Bailey, M., Tatton, B. L., et al. 2013, A&A, 550, A108

Vergely, J.-L., et al. 2001, A&A, 366, 1016

Vergely, J.-L., et al. 2010, A&A, 518, A31

Welsh, B. Y., et al. 2010, A&A, 510, A54

Wolff, B., Koester, D., & Lallement, R. 1999, A&A, 346, 969

Wood, B. E., Linsky, J. L., Hébrard, G. 2004, ApJ, 609, 838